PLOS ONE

RESEARCH ARTICLE

Genetic deletion of calcium-independent phospholipase $A_2\gamma$ protects mice from diabetic nephropathy

Andrey V. Cybulsky[1]*, Joan Papillon[1], Julie Guillemette[1], José R. Navarro-Betancourt[1], Hanan Elimam[2], I. George Fantus[1]

1 Department of Medicine, McGill University Health Centre, McGill University, Montreal, Quebec, Canada,
2 Department of Biochemistry, Faculty of Pharmacy, University of Sadat City, Sadat City, Egypt

* andrey.cybulsky@mcgill.ca

Citation: Cybulsky AV, Papillon J, Guillemette J, Navarro-Betancourt JR, Elimam H, Fantus IG (2024) Genetic deletion of calcium-independent phospholipase $A_2\gamma$ protects mice from diabetic nephropathy. PLoS ONE 19(10): e0311404. https://doi.org/10.1371/journal.pone.0311404

Editor: Partha Mukhopadhyay, National Institutes of Health, UNITED STATES OF AMERICA

Received: May 27, 2024

Accepted: September 18, 2024

Published: October 31, 2024

Data Availability Statement: All relevant data are within the manuscript and its Supporting Information files.

Funding: This work was supported by Research Grants from the Canadian Institutes of Health Research (PJ9-166216 and PJ9-169678; to AVC), www.cihr-irsc.gc.ca, and the Kidney Foundation of Canada (to AVC), www.kidney.ca, and the Catherine McLaughlin Hakim Chair (to AVC). The funders had no role in study design, data collection

Abstract

Calcium-independent phospholipase $A_2\gamma$ ($iPLA_2\gamma$) is localized in glomerular epithelial cells (GECs)/podocytes at the mitochondria and endoplasmic reticulum, and can mediate release of arachidonic acid and prostanoids. Global knockout (KO) of $iPLA_2\gamma$ in mice did not cause albuminuria, but resulted in mitochondrial structural abnormalities and enhanced autophagy in podocytes. In acute glomerulonephritis, deletion of $iPLA_2\gamma$ exacerbated albuminuria and podocyte injury. This study addresses the role of $iPLA_2\gamma$ in diabetic nephropathy. Hyperglycemia was induced in male mice with streptozotocin (STZ). STZ induced progressive albuminuria in control mice (over 21 weeks), while albuminuria did not increase in $iPLA_2\gamma$ KO mice, remaining comparable to untreated groups. Despite similar exposure to STZ, the STZ-treated $iPLA_2\gamma$ KO mice developed a lower level of hyperglycemia compared to STZ-treated control. However, there was no significant correlation between the degree of hyperglycemia and albuminuria, and even $iPLA_2\gamma$ KO mice with greatest hyperglycemia did not develop significant albuminuria. Mortality at 21 weeks was greatest in diabetic control mice. Sclerotic glomeruli and enlarged glomerular capillary loops were increased significantly in diabetic control compared to diabetic $iPLA_2\gamma$ KO mice. Glomerular matrix was expanded in diabetic mice, with control exceeding $iPLA_2\gamma$ KO. Glomerular autophagy (increased LC3-II and decreased p62) was enhanced in diabetic $iPLA_2\gamma$ KO mice compared to control. Treatment of cultured GECs with H_2O_2 resulted in increased cell death in control GECs compared to $iPLA_2\gamma$ KO, and the increase was slightly greater in medium with high glucose compared to low glucose. H_2O_2-induced cell death was not affected by inhibition of prostanoid production with indomethacin. In conclusion, mice with global deletion of $iPLA_2\gamma$ are protected from developing chronic glomerular injury in diabetic nephropathy. This is associated with increased glomerular autophagy.

Introduction

Among human glomerular diseases, diabetic nephropathy (DN) is a leading cause of chronic kidney disease, and has a major impact on health [1, 2]. Current therapies of glomerulopathies

and analysis, decision to publish, or preparation of the manuscript.

Competing interests: The authors have declared that no competing interests exist.

and diabetic nephropathy are only partially effective, display significant toxicities and lack specificity [1]. Thus, it is important to understand the mechanisms of glomerular diseases to develop mechanism-based therapies.

Podocytes or glomerular visceral epithelial cells (GECs) are functionally important in the sustenance of glomerular permselectivity [3, 4]. The structure of podocytes is complex–the cells display cell bodies with projecting interdigitating foot processes that are connected by filtration slit-diaphragms. The elaborate shape of podocytes is supported by the actin cytoskeleton. Podocytes synthesize slit-diaphragm and adhesion proteins, as well as glomerular basement membrane (GBM) components; consequently, these cells are metabolically active with high energy demands. Podocyte injury, characterized by albuminuria, is a prominent feature of glomerular diseases, including diabetic nephropathy [3–5].

Calcium-independent phospholipase A$_2$γ (iPLA$_2$γ) catalyzes cleavage of fatty acids from the sn-1 or sn-2 position of phospholipids and from other substrates, such as cardiolipin [6]. We showed that iPLA$_2$γ mRNA and protein are expressed in the glomerulus in vivo [7]. In complement-mediated GEC injury, iPLA$_2$γ promoted cytoprotection [7]. Global knockout (KO) of iPLA$_2$γ in mice results in prominent mitochondrial ultrastructural abnormalities in podocytes, increases autophagosomes in these cells, and leads to depletion of podocytes in aging mice (although without albuminuria) [5, 8]. There were, however, no mitochondrial abnormalities or increased autophagosomes in mesangial and glomerular endothelial cells [8]. In experimental anti-GBM nephritis, and experimental focal segmental glomerulosclerosis (adriamycin nephrosis), KO of iPLA$_2$γ worsened albuminuria [5, 8]. Therefore, iPLA$_2$γ has a protective action in the normal glomerulus and in glomerulonephritis. In addition, our work in cultured GECs confirmed that loss of iPLA$_2$γ leads to mitochondrial dysfunction and increased autophagy [5, 8].

We and others showed that in cells, iPLA$_2$γ is found at the endoplasmic reticulum and mitochondria, and this localization is regulated by the N-terminal region of iPLA$_2$γ [5, 6, 9–11]. iPLA$_2$γ can be active constitutively or can be stimulated [6]; stimulation of iPLA$_2$γ activity by complement was due to phosphorylation at Ser-511 and/or Ser-515 via mitogen-activated protein kinase-interacting kinase 1 (MNK1) [10]. iPLA$_2$γ can also be activated by oxidative stress [12], and it can affect the endoplasmic reticulum unfolded protein response [13]. Phospholipases located at the mitochondria are reported to regulate mitochondrial function and signaling pathways [6, 11]. Global deletion of iPLA$_2$γ in mice altered cardiolipin content and molecular species distribution that was accompanied by defects in mitochondrial function [14]. Studies have revealed a role for iPLA$_2$γ in mitochondrial function and cellular energy metabolism in various organs, including heart, skeletal muscle, adipose tissue, liver, and brain [5, 14–18]. iPLA$_2$γ global KO mice display reduced growth rate, cold intolerance and bioenergetic dysfunction [15]. In the brains of aging mice with global iPLA$_2$γ deletion, there was disruption of mitochondrial phospholipid homeostasis, presence of enlarged and degenerating mitochondria, increased autophagy and cognitive dysfunction [16]. Deletion of iPLA$_2$γ in skeletal muscle resulted in muscle mitochondrial dysfunction and atrophy [19].

On the other hand, KO of iPLA$_2$γ attenuated calcium-induced opening of the mitochondrial permeability transition pore and cytochrome c release [14]. Mice with myocardial KO of iPLA$_2$γ showed less production of proinflammatory oxidized fatty acids, and developed substantially less cardiac necrosis compared with wild type littermates following ischemia-reperfusion injury [20]. In failing hearts, increased iPLA$_2$γ activity channeled arachidonic acid into toxic hydroxyeicosatetraenoic acids (HETEs), promoting mitochondrial permeability transition pore opening, inducing myocardial necrosis/apoptosis and leading to further progression of heart failure [21]. Hepatic KO of iPLA$_2$γ in mice subjected to high fat diet increased iPLA$_2$γ-mediated hepatic 12-HETE production leading to mitochondrial dysfunction and

hepatocyte death [22]. Deletion of iPLA$_2$γ also reduced colonic tumorigenesis and venous thromboembolism [6]. Thus, iPLA$_2$γ is critical in mitochondrial lipid metabolism and maintenance of membrane structure. Loss of iPLA$_2$γ perturbs fatty acid β-oxidation, oxygen consumption, energy expenditure, and tissue homeostasis [5]. However, the outcomes of iPLA$_2$γ activity may be deleterious or protective depending on the context.

A small number of humans with mutations in the gene encoding iPLA$_2$γ (PNPLA8) have been described. Phenotypes have included mitochondrial myopathy, lactic acidosis, microcephaly, seizures, neurodegeneration and ataxia; most cases have been severe, but two individuals survived into adulthood [23, 24]. There is no information on renal phenotype.

The mechanisms and pathogenesis of diabetic nephropathy are complex and poorly understood [25–27]. Briefly, hyperglycemia and oxidative stress stimulate diacylglycerol, protein kinase C, the polyol pathway and advanced glycation end products, leading to protein glycosylation and stimulation of inflammatory mediators/cytokines and growth factors. This leads to renal hemodynamic changes and structural damage, in particular to podocytes, and podocyte injury is key in the pathogenesis of diabetic nephropathy [25, 28–30]. A widely used experimental model of type 1 diabetes in rodents is induced by streptozotocin (STZ), a chemical toxin for pancreatic β-cells. Renal injury resembles human diabetic nephropathy, and it includes albuminuria, podocyte loss, mesangial and GBM expansion, and decline in kidney function. Eventually, this progresses to glomerular and tubulointestitial sclerosis, although a limitation of the model is that injury is relatively mild [27, 28, 31]. In the present study, we address the role of iPLA$_2$γ in diabetic nephropathy–a clinically-important cause of glomerular injury, whose pathogenesis is distinct from the primary/acute glomerulopathies. In contrast to acute glomerulonephritis, mice with global deletion of iPLA$_2$γ are protected from developing chronic glomerular injury in diabetic nephropathy.

Materials and methods

Antibodies and chemicals

Goat anti-synaptopodin antibody (sc-21537) was purchased from Santa Cruz Biotechnology (Santa Cruz, CA). Rabbit anti-Wilms tumor-1 (WT1) antibody (CAN-R9(IHC)-56-2; ab89901) was from Abcam Inc. (Toronto, ON). Rat anti-collagen α5 (IV) antibody, clone H53 (7078) was purchased from Chondrex Inc. (Woodinville, WA). Rabbit antibodies to LC3B (2775) and SQSTM1/p62 (5114) were purchased from Cell Signaling Technology (Danvers, MA). Mouse anti-LC3B clone 5F10 (ALX-830-080-C100) was from Enzo Life Sciences (Ann Arbor, MI). Rabbit anti-ubiquitin (U5379) and rabbit anti-actin (A2066) antibodies were from MilliporeSigma (Mississauga, ON). Rat anti-mouse F4/80 antibody MCA497GA was from Bio-Rad (Mississauga, ON). Goat anti-podocalyxin antibody (AF1556) was purchased from R & D Systems (Minneapolis, MN). Rabbit anti-nephrin antiserum was a gift from Dr. Tomoko Takano (McGill University) [32]. Non-immune IgG and secondary antibodies were from Jackson ImmunoResearch Laboratories (West Grove, PA) or Thermo-Fisher Scientific. Streptozotocin (STZ) and rhodamine-phalloidin were from MilliporeSigma. 5(6)-Carboxy-2′,7′-dichlorofluorescein diacetate N-succinimidyl ester (DCF) was from Santa Cruz Biotechnology.

Studies in mice (in vivo)

iPLA$_2$γ global KO mice in a C57BL/6 background were kindly provided by Dr. Richard Gross (Washington University, St. Louis, MO, USA). Mice were produced, bred and genotyped, as described previously [8, 15]. The animals were housed in a pathogen free facility, under standard conditions including cages and bedding, with 12 h on-off light cycles, and were fed ad libitum. Adult (6 month old) male control and iPLA$_2$γ KO littermates were untreated or

received STZ 50 mg/kg (in 50 mM sodium citrate buffer, pH 4.5) intraperitoneally daily for 5 days [31]. Mice were given 10% sucrose water to drink for 6 days after STZ treatment to prevent fatal hypoglycemia. The animals were randomly allocated to experimental groups. Blood glucose was measured after 1 week using glucose test strips. If hyperglycemia did not develop, the protocol, was repeated. This low-dose STZ protocol avoids direct STZ renal toxicity. Mice were followed for ~6 months and were euthanized (isofluorane followed by cervical dislocation) in the animal facility to collect the kidneys and isolate glomeruli by sequential sieving [8]. The animal protocol was approved by the McGill University Animal Care Committee (MUHC-4625 and 10086), and our studies comply with the guidelines established by the Canadian Council on Animal Care. The study complied with ARRIVE guidelines.

Urine collections were performed in the morning in the animal facility at ~4-week intervals until the mice were euthanized. Urine albumin was quantified with an enzyme-linked immunosorbent assay (Mouse Albumin ELISA Quantification Kit, Bethyl Laboratories, Montgomery, TX). Albumin results were normalized to urine creatinine, which was measured using a picric acid-based reaction (Creatinine Colorimetric Assay Kit, Cayman Chemical Co; Ann Arbor, MI) [8, 32].

Studies in cell culture

Primary GECs were derived from iPLA$_2$γ KO mice and wild type control mice [5, 13]. The detailed method and characterization of the cells was published previously [13]. Control and iPLA$_2$γ KO cell lines were cultured on plastic substratum in K1 medium (DMEM, Ham F-12, with 5% NuSerum and hormone mixture). For experiments, GECs were allowed to proliferate for one day at 33˚C and were then switched to 37˚C to differentiate for 24 h. The lactate dehydrogenase (LDH) release assay to assess cell death was described previously [7, 8].

Microscopy

For light microscopy, portions of kidneys were fixed in 4% paraformaldehyde and stained with periodic acid-Schiff by conventional techniques at the McGill University Health Centre Histology Platform. To minimize observer bias, quantitative morphometry was used to characterize histological changes. Slides were digitized at 40x resolution in an Aperio AT Turbo scanner (Leica Biosystems, Buffalo Grove, IL). Images were processed using Aperio ImageScope 12.4 (Leica Biosystems). Glomeruli in experimental groups were selected randomly and analyzed with the Positive Pixel Count v9 algorithm, as reported previously [32]. Positive pixels were identified by a hue value of 0.854 (pink) and a hue width of 0.035. Glomerular matrix expansion was expressed as the ratio of positive over total pixels. To quantify podocyte number (WT1 counts) and kidney macrophages (F4/80 staining), kidney sections were deparaffinized and rehydrated. Antigen retrieval was done using citrate buffer, pH 6. Automated immunohistochemistry staining was performed by the McGill University Health Centre Histology Platform, using the Discovery Ultra Instrument (Roche Diagnostics). For WT1, the WT1-positive nuclei were then quantified by visual counting.

For immunofluorescence (IF) microscopy, kidney poles were snap-frozen in isopentane (-80˚C). Cryostat sections (4 μm thickness) were cut and then fixed in 4% paraformaldehyde (22˚C), ice-cold methanol or ice-cold acetone, and blocked with 5% normal rabbit or goat serum or 3–5% BSA. Incubations with primary antibodies were performed overnight at 4˚C, and incubations with secondary antibodies were 1 h at 22˚C. In control incubations (performed in parallel), primary antibody was replaced with nonimmune IgG. In some experiments, cell nuclei were stained with Hoechst H33342 [32, 33]. Glomeruli in experimental groups were selected randomly and images were acquired using a Zeiss Axio Observer Z1

LSM780 laser scanning confocal microscope with ZEN2010 software (McGill University Health Centre Research Institute Imaging Platform). To compare fluorescence intensities, all images were taken at the same exposure time. Fluorescence intensity was quantified using the histogram function of ImageJ software (National Institutes of Health, Bethesda, MD), and results are expressed in arbitrary units [32, 33]. The glomerular fluorescence intensity was normalized to the total fluorescence in each image. To measure the colocalization of two proteins in mouse kidney sections, glomeruli were circled, and threshold intensity of each channel was measured, as previously. Colocalization of the thresholded images in kidney sections was determined using the JACoP plugin in ImageJ [33].

Immunoblotting

The immunoblotting protocol was described previously [8, 32]. Chemiluminescence was measured in a ChemiDoc Touch Imaging System (Bio-Rad; Mississauga, ON) [32]. Signal saturation was monitored with Image Lab (Bio-Rad) and only signal intensities within a linear range were analyzed. Densitometry of bands was quantified using ImageJ, and values were normalized to the expression of β-actin.

Statistical analysis

Values are expressed as mean ± standard error or as the median where indicated. Data were processed in Prism (GraphPad Software, La Jolla, CA). In experiments with three or more groups, or groups and multiple time-points, one-way or two-way analysis of variance (ANOVA) was used to determine significant differences among groups; where relevant, additional comparisons were calculated and values were adjusted according to the Holm-Sidak method. In certain cases, where the data were not normally distributed and the number of replicates was <20, we used the Kruskal-Wallis test. In experiments with two groups, the Mann Whitney U test was used. Significant differences between two groups are displayed with lines between columns, with asterisks denoting P values. In the absence of such lines, differences were not statistically significant. Statistical tests are presented in the figure legends.

Results

KO of iPLA$_2$γ attenuates development of albuminuria in STZ-diabetic nephropathy

Mice with global deletion of iPLA$_2$γ (mean age 6.5 months) were employed to address the functional role of iPLA$_2$γ in STZ-induced diabetic nephropathy. Within one month after treatment of mice with STZ, increases in blood glucose were evident in both control and iPLA$_2$γ KO mice, indicating development of diabetes (S1 Fig). STZ induced significant increases in glucose in both control and iPLA$_2$γ KO mice; however, mean glucose levels over the study period were greater in control mice. Adult iPLA$_2$γ KO mice are known to be smaller than wild type mice [15, 16, 22]. In keeping with this, untreated and STZ-treated iPLA$_2$γ KO mice showed lower body weights compared to untreated and STZ-treated controls. Furthermore, STZ-treated control mice showed lower body weight compared to untreated control, whereas the weight of STZ-treated iPLA$_2$γ KO mice did not decrease further below the already smaller untreated iPLA$_2$γ animals (S1 Fig).

Induction of diabetes induced progressive albuminuria in control mice, and the albuminuria in diabetic control mice was significantly greater compared to diabetic iPLA$_2$γ KO mice (the week 2–21 time points were considered together in the analysis). Diabetic iPLA$_2$γ KO mice showed slightly although not significantly greater albuminuria compared to untreated

iPLA$_2$γ KO mice, and the levels of albuminuria in these KO mice were comparable to untreated control (Fig 1A).

Since blood glucose levels were greater in diabetic control mice compared to iPLA$_2$γ KO, we removed 7 mice from analysis of the iPLA$_2$γ KO group. This resulted in an increase in the mean blood glucose in the remaining subgroup of diabetic iPLA$_2$γ KO mice (S1 Fig); however, the mean urine albumin/creatinine values at all time points did not change significantly and remained substantially lower compared to diabetic controls (S2 Fig). Indeed, there was a weak correlation between the mean albumin/creatinine value of each diabetic mouse and mean blood glucose value of the same mouse in both the control and iPLA$_2$γ KO groups (Fig 1). Finally, the greatest mortality was evident in the diabetic control mice (Fig 1).

Diabetic control mice show alterations in glomerular morphology

Mouse kidneys were isolated after 21 weeks of diabetes. Both diabetic control and iPLA$_2$γ KO mice showed increases in glomerular matrix, compared to the respective untreated groups. Furthermore, the increase was significantly greater in control mice (Fig 2). Glomerular cross-sectional area was not substantially different among groups of mice, although statistically, it was reduced slightly in diabetic iPLA$_2$γ KO mice compared to untreated iPLA$_2$γ KO (Fig 2).

Kidney sections were immunostained with antibodies to the podocyte protein synaptopodin and collagen IV-α5. Importantly, diabetic control mice showed an increase in sclerotic glomeruli, and although there was no change in glomerular area, the diabetic control glomeruli showed large capillary loops, compared to the other groups (Fig 3). The latter is compatible with reduced glomerular contractility and glomerular hypertension/hyperfiltration.

The presence of albuminuria in diabetic control mice reflects podocyte injury. However, we did not observe a loss of podocytes, i.e. there were no significant differences in WT1 counts (podocyte numbers) or WT1/glomerular area counts among groups (Fig 4). In addition, there were no significant differences in the podocyte protein synaptopodin or glomerular collagen IV-α5 immunofluorescence staining intensities among groups (Fig 3). Colocalization of synaptopodin and collagen IV-α5 was not substantially different among groups. The Pearson correlation coefficients were 0.67±0.05 (untreated control), 0.72±0.05 (untreated iPLA$_2$γ KO), 0.69±0.08 (diabetic control) and 0.66±0.04 (diabetic iPLA$_2$γ KO). These values imply that most of the collagen IV-α5 was localized in or near podocytes. Finally, glomeruli were isolated from mouse kidneys and lysates were subjected to immunoblotting to examine expression of nephrin and podocalyxin. There were no significant differences in the expression of these proteins among groups (S3 Fig).

The complex structure of podocytes, in particular their foot processes is dependent on the actin cytoskeleton [3, 4]. To examine the effect of iPLA$_2$γ and diabetes on actin cytoskeleton organization in podocytes, kidney sections were stained with phalloidin (which labels F-actin) and synaptopodin [34]. Confocal fluorescence microscopy demonstrated substantial colocalization of F-actin and synaptopodin (Pearson colocalization coefficient >0.75). In keeping with our findings on WT1 counts and expression of podocyte proteins, glomerular F-actin content (phalloidin fluorescence intensity) and F-actin colocalization with synaptopodin did not show significant differences among the groups of mice, implying that deletion of iPLA$_2$γ and diabetes did not substantially affect cytoskeleton organization and foot processes (S4 Fig).

Inflammatory cells in diabetic kidneys

Diabetic nephropathy may represent a proinflammatory condition associated with infiltration of inflammatory cells [25, 35]. To examine for macrophages, kidney sections were stained with the F4/80 macrophage-specific antibody. There was only minimal F4/80 staining in the 4

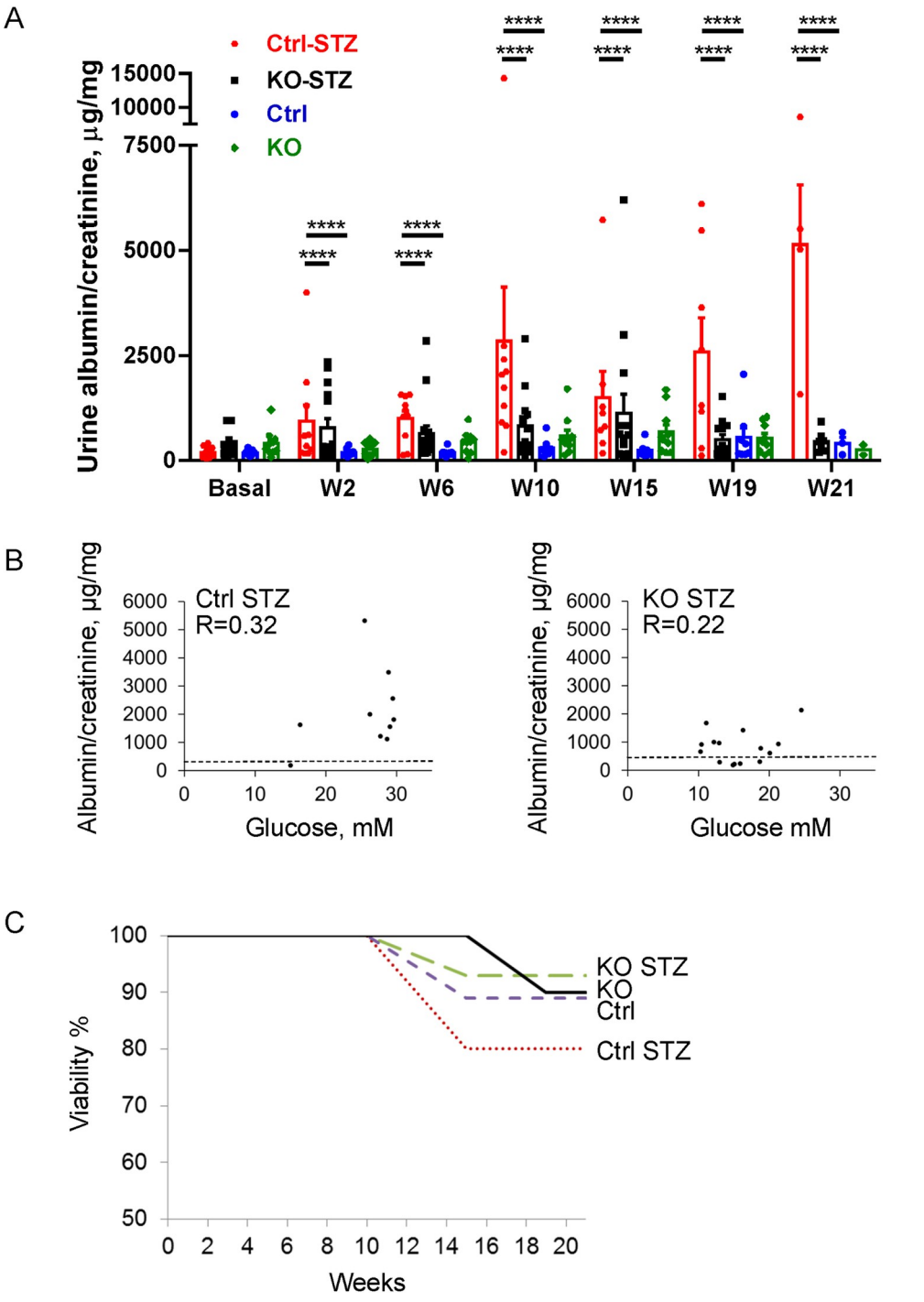

Fig 1. KO of iPLA$_2$γ attenuates development of albuminuria in STZ-induced diabetic nephropathy. A) Treatment of mice with STZ induces progressive albuminuria (monitored as urine albumin/creatinine) in control mice. N = 9 mice in control (Ctrl) untreated (Untr), 10 in KO Untr, 10 in Ctrl STZ and 15 in KO STZ groups. ****P<0.0001 Ctrl STZ vs KO STZ, P<0.0001 Ctrl STZ vs Ctrl untreated. KO Untr vs KO STZ is not significant (the week 2–21 time points were considered together in the analysis; two-way ANOVA). W, week. B) Albuminuria does not correlate with blood glucose. The mean week 2–21 albumin/creatinine value of each diabetic mouse are plotted against mean blood glucose value of the same mouse. The correlations in each group are relatively weak (P values are not significant). The dashed lines indicate the mean urine albumin/creatinine values of the respective untreated groups. C) Viability of mice. Greatest mortality is evident in the Ctrl STZ mice.

https://doi.org/10.1371/journal.pone.0311404.g001

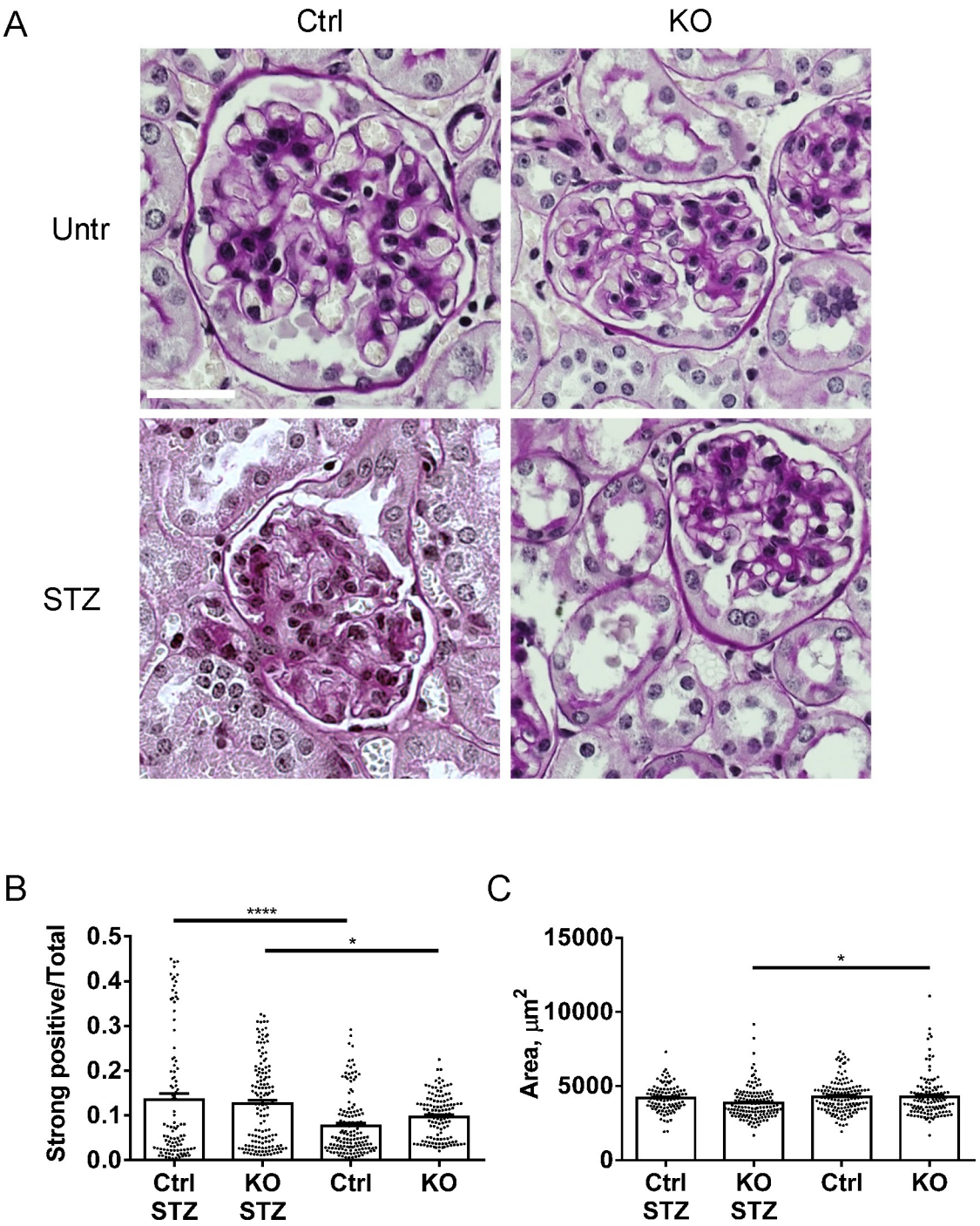

Fig 2. STZ increases glomerular matrix expansion. Kidney sections were stained with periodic acid-Schiff and glomerular matrix expansion was evaluated with a pixel-counting algorithm. A) Representative photomicrographs. B) Quantification of extracellular matrix. Both STZ-treated control and iPLA$_2$γ KO mice show significant increases in glomerular matrix, compared to untreated groups, and the increase is greater in control ($P<0.02$). C) Glomerular cross-sectional area is reduced slightly in iPLA$_2$γ KO STZ compared to KO untreated mice and tends to be slightly lower in control STZ compared to control untreated. 20 glomeruli in 5–6 mice per group were analyzed. *$P<0.05$, ****$P<0.0001$ (ANOVA). Bar = 25 μm (all panels are presented at the same magnification).

https://doi.org/10.1371/journal.pone.0311404.g002

Figure 3

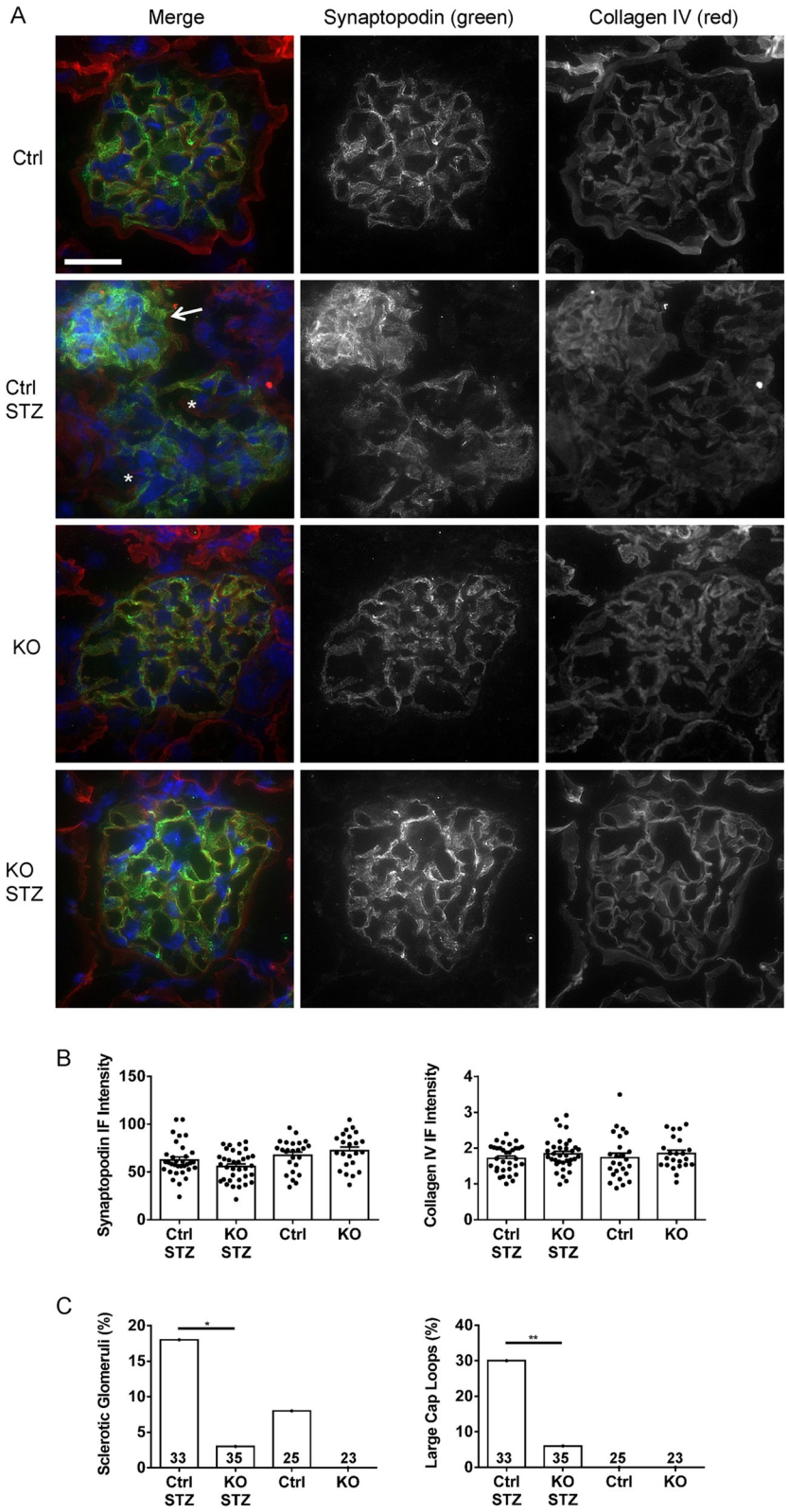
A
Merge
Synaptopodin (green)
Collagen IV (red)
Ctrl
Ctrl STZ
KO
KO STZ
B
Synaptopodin IF Intensity
Collagen IV IF Intensity
Ctrl STZ
KO STZ
Ctrl
KO
C
Sclerotic Glomeruli (%)
Large Cap Loops (%)
33
35
25
23
*
**

Fig 3. Control (Ctrl) STZ mice show changes in glomerular morphology. A) Kidney sections were stained with antibodies to synaptopodin and collagen IV-α5 (representative immunofluorescence micrographs). B) Quantification of immunofluorescence intensity. There are no significant differences in synaptopodin or collagen immunofluorescence intensities among groups (ANOVA). However, Ctrl STZ mice show an increase in sclerotic glomeruli (A; arrow) and glomeruli with large capillary loops (*) compared to the other groups (quantification in panel C). 5–7 glomeruli/mouse in 4–6 mice per group were analyzed. *P<0.05, **P<0.01 (Chi-squared test). Bar = 25 μm.

https://doi.org/10.1371/journal.pone.0311404.g003

groups of mice, suggesting that macrophages were largely absent (S5 Fig). Periodic acid-Schiff-stained slides were also examined for the presence of neutrophils. Occasional neutrophils were visualized in the kidney sections, but the numbers were very small and did not allow for accurate quantification (S6 Fig).

Autophagy is enhanced in iPLA$_2$γ KO mice

Protein misfolding and impaired clearance of misfolded proteins in glomerular cells, particularly podocytes may contribute to podocyte injury in glomerulopathies [36]. In this set of experiments, we examined the effects of iPLA$_2$γ and diabetes on pathways of protein

Figure 4

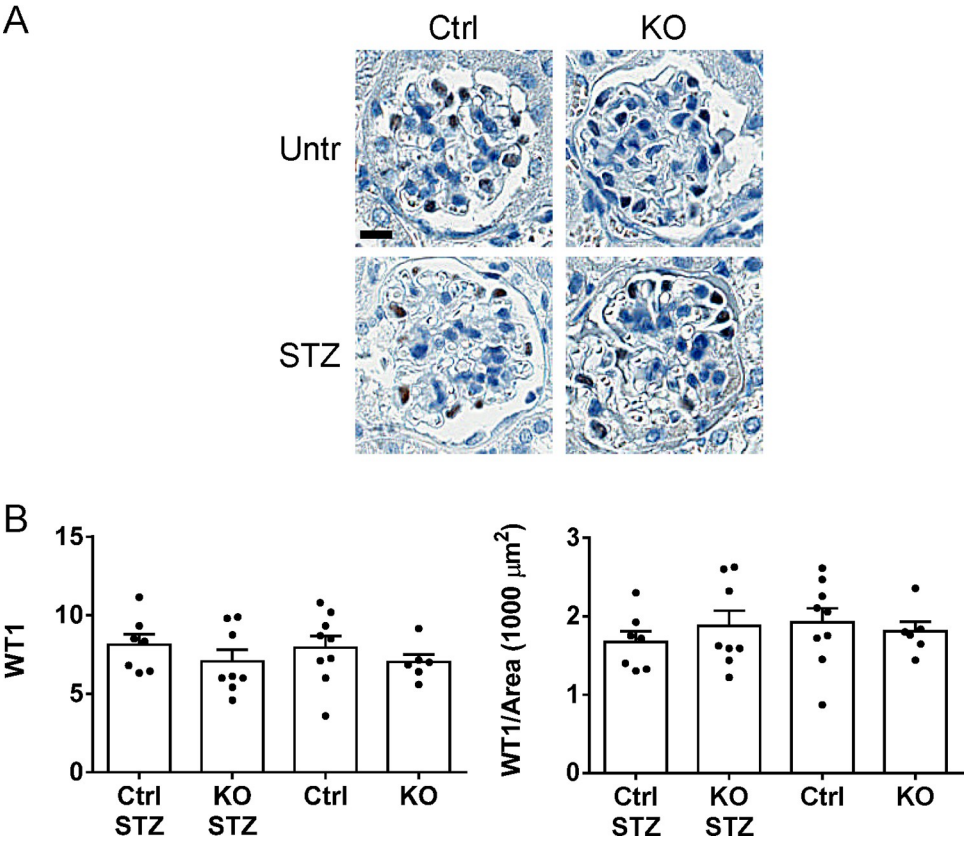

Fig 4. Podocyte numbers in control and iPLA$_2$γ KO mice (WT1-positive cells). A) Kidney sections were stained with anti-WT1 antibody (representative photomicrographs). B) WT1 counts. There are no significant differences in WT1 counts or WT1/glomerular area counts among groups (ANOVA). 10 glomeruli/mouse in 5–7 mice per group were analyzed; each point is the mean value of a single mouse. Bar = 25 μm.

https://doi.org/10.1371/journal.pone.0311404.g004

degradation. Among these, autophagy is a prominent pathway that regulates protein homeostasis in podocytes [36]. Lysates of glomeruli isolated after 21 weeks of diabetes were immunoblotted with anti-LC3 or anti-p62 antibodies [5, 8, 32]. LC3-II, a marker of autophagy, was increased significantly in untreated and diabetic iPLA$_2$γ KO mice compared to untreated and diabetic control (Fig 5). p62 (an autophagy substrate) was decreased in diabetic iPLA$_2$γ KO mice compared to the other groups (Fig 5), implying enhanced degradation of p62 by autophagy in the diabetic iPLA$_2$γ KO mice. Thus, autophagy was enhanced in diabetic iPLA$_2$γ KO mice, while untreated iPLA$_2$γ KO may have higher basal autophagy. In the diabetic iPLA$_2$γ KO mice, autophagy correlated with lower albuminuria, and could thus represent a protective pathway.

To address protein degradation via the ubiquitin-proteasome system [5, 36], lysates were immunoblotted with anti-ubiquitin antibody. In contrast to LC3-II, there were no significant differences in protein ubiquitination among groups (Fig 5), suggesting there were no substantial differences in the function of the ubiquitin-proteasome system.

Control GECs are more susceptible to injury compared to iPLA$_2$γ KO GECs

As discussed above, diabetic control mice showed greater albuminuria compared to iPLA$_2$γ KO mice (Fig 1). Therefore, we examined if cultured GECs derived from control mice are more susceptible to injury compared to GECs from iPLA$_2$γ KO mice. GECs were untreated, or treated with potentially cytotoxic compounds, including tunicamycin, adriamycin or H_2O_2. To reflect the diabetic environment in vivo, experiments were carried out in medium with a high glucose concentration (36 mM); low glucose medium was used as control (7.8 mM). By analogy to an approach employed in hepatocytes [22], injury was assessed by monitoring release of LDH from cells into cell supernatants. Control GECs were more susceptible to adriamycin- and H_2O_2-induced cytolysis compared to iPLA$_2$γ KO GECs (Fig 6A), thus recapitulating injury in vivo. Furthermore, in control GECs, H_2O_2-induced cytolysis was greater in high glucose medium compared to low glucose. Adriamycin-induced cytolysis in control GECs was slightly greater in high glucose medium compared to low glucose, but the difference did not reach statistical significance. Similarly to H_2O_2, adriamycin induces cytotoxicity via production of reactive oxygen species, but adriamycin can also activate other cytotoxic pathways that are less dependent on a high glucose milieu. Tunicamycin was not cytotoxic at the doses employed.

iPLA$_2$γ was shown to induce production of prostanoids in GECs [10]. Thus, we examined if inhibition of free arachidonic acid metabolism via cyclooxygenase would affect cytolysis. Control GECs in high glucose medium were untreated or treated with indomethacin, adriamycin, H_2O_2, adriamycin + indomethacin, or H_2O_2 + indomethacin. No significant effects of indomethacin on modulating cytotoxicity were observed (Fig 6B). Glomeruli have been reported to express 12/15-lipoxygenase [37, 38]. Thus, by analogy to cyclooxygenase, we tested if the 5- and 12/15-lipoxygenase inhibitor nordihydroguaiaretic acid (0.25–0.5 μM) and the 12/15-lipoxygenase inhibitor baicalein (10 μM) would modulate cytotoxicity in control GECs. Nordihydroguaiaretic acid proved to be independently toxic to GECs and could not be evaluated further. Baicalein reversed H_2O_2-induced LDH release in low and high glucose media, but the effect of baicalein was similar in both control and iPLA$_2$γ KO GECs. Therefore, it cannot be concluded that the apparent cytoprotective effect of baicalein was associated with iPLA$_2$γ.

Production of reactive oxygen species

Reactive oxygen species may be generated in glomerular cells under diabetic conditions, and can be potentially cytotoxic [25]. We assayed production of reactive oxygen species in control

Figure 5

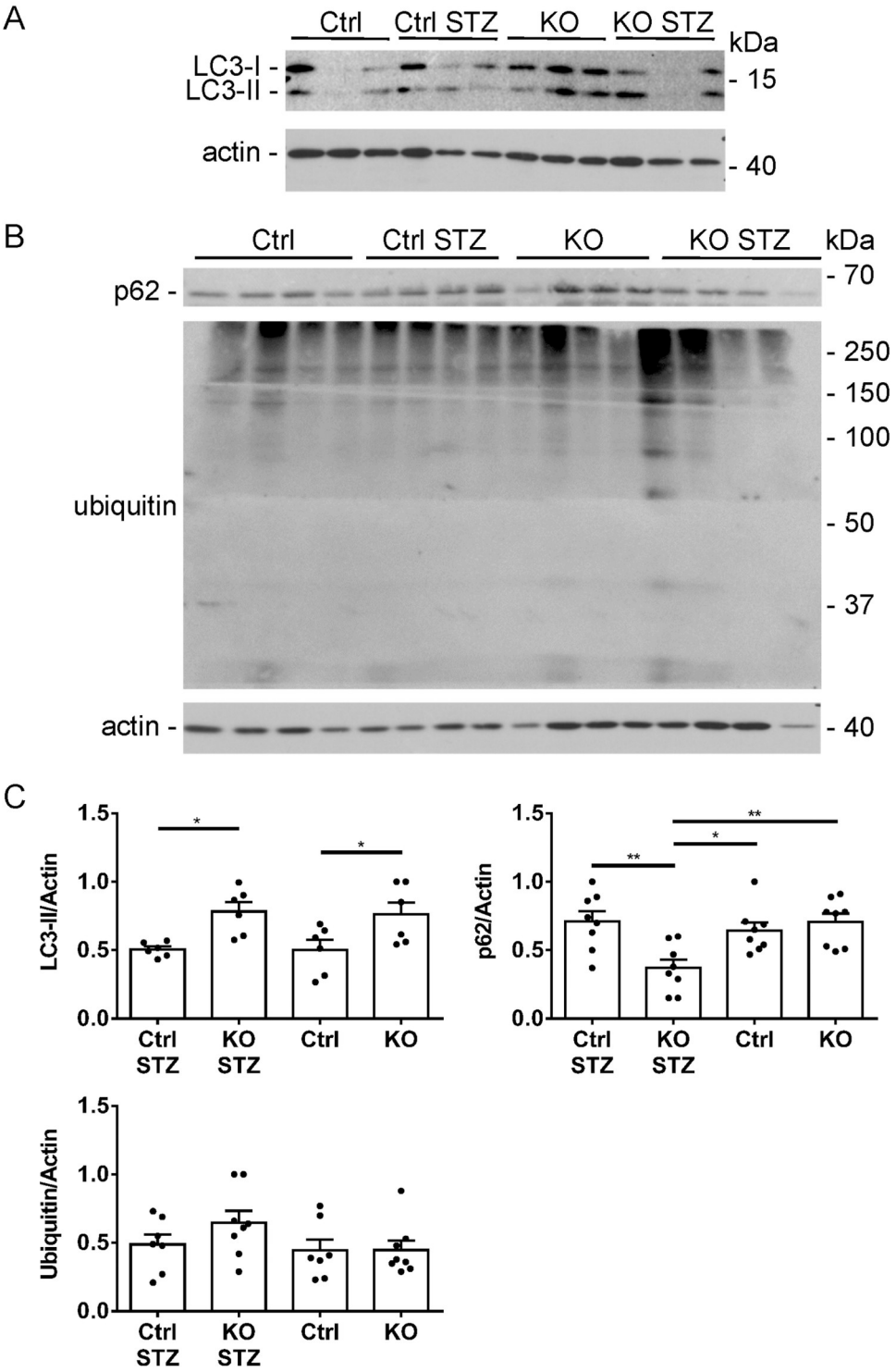

Fig 5. iPLA$_2$γ KO mice show increased glomerular autophagy. A and B) Glomerular lysates were immunoblotted with antibodies to LC3, p62 and ubiquitin (representative immunoblots). C) Signals were quantified by densitometry. LC3-II is increased significantly in untreated and STZ-treated iPLA$_2$γ KO mice compared to untreated and STZ-

treated control. p62 is decreased significantly in STZ-treated iPLA$_2$γ KO mice. There are no significant differences in protein ubiquitination among groups. There are 6–8 mice per group. *P<0.05, **P<0.01 (ANOVA).

https://doi.org/10.1371/journal.pone.0311404.g005

and iPLA$_2$γ KO GECs under hyperglycemic conditions using 2',7'-dichlorodihydrofluorescein diacetate (DCF) fluorescence. Cells were cultured in medium containing 7.8 mM glucose. Then, medium was switched to 7.8 mM glucose + 28 mM mannitol (Man) or high glucose (36 mM) for 24 h. DCF was added and fluorescence was measured after 15 min. Although DCF fluorescence appeared to be greater in high glucose, there were no significant differences in DCF fluorescence between high and low glucose groups, nor between control and iPLA$_2$γ KO GECs (S7 Fig). The results suggest that endogenous production of reactive oxygen species, such as H_2O_2 is unlikely to mediate cytotoxicity in cultured GECs.

Autophagy in cultured GECs

As shown in Fig 5, LC3-II, reflecting autophagy, was enhanced in glomeruli of untreated and diabetic iPLA$_2$γ KO mice. First, we confirmed results reported previously [5, 8], showing that basal levels of LC3-II (monitored by immunoblotting) were greater in cultured iPLA$_2$γ KO GECs compared to control (0.29±0.07 units in KO GECs vs 0.11±0.04 units in control; by densitometry; P = 0.04, 8 experiments performed in duplicate). Next, we examined if high glucose could modulate autophagy in GECs. Cells were cultured in low glucose medium. Then, incubations were continued in low glucose + mannitol or high glucose for 24 h, and in addition, cells were treated with or without chloroquine (chloroquine blocks autophagic flux). LC3-II increased significantly after addition of chloroquine in control and iPLA$_2$γ KO cells exposed to mannitol or high glucose, but there were no significant differences among these 4 groups (S8 Fig).

Finally, we tested if inhibition of autophagy would enhance cytotoxicity. Using control GECs, we tested two compounds that have been reported to inhibit autophagy, including the ULK1 inhibitor SBI0206965 and the VPS34 kinase activity inhibitor SAR405 [39]. SBI0206965 reduced tunicamycin-induced LC3-II production, while SAR405 was not effective (S8 Fig). Then, we incubated GECs with H_2O_2 in the presence or absence of SBI0206965 (we used a 2.5 μM dose, since higher doses showed some drug-dependent cytotoxicity). SBI0206965 augmented H_2O_2-induced LDH release in both control and iPLA$_2$γ KO GECs to a similar extent (Fig 6C), supporting the view that autophagy is a cytoprotective mechanism in GECs.

Discussion

The present study demonstrates that deletion of iPLA$_2$γ attenuates development of albuminuria in STZ-induced diabetic nephropathy. While albuminuria in diabetic iPLA$_2$γ KO mice tended to be greater than levels in the untreated iPLA$_2$γ KO group, the difference was not statistically significant. iPLA$_2$γ KO mice were more resistant to developing hyperglycemia compared to control mice. Nevertheless, when analyzing the subset of iPLA$_2$γ KO mice with greatest hyperglycemia, even this group did not show a significant increase in albuminuria, and there was only weak correlation between albuminuria and blood glucose in individual mice. Consistent with albuminuria, diabetic control mice demonstrated a higher mortality compared to the other experimental groups.

The lower blood glucose levels in iPLA$_2$γ KO mice is in keeping with earlier studies, which showed that during high fat feeding, mice with global, hepatic and skeletal muscle KO of iPLA$_2$γ demonstrated improved glucose tolerance and enhanced blood glucose clearance relative to controls [18, 19, 22]. Previously, it was shown that control mice released more insulin

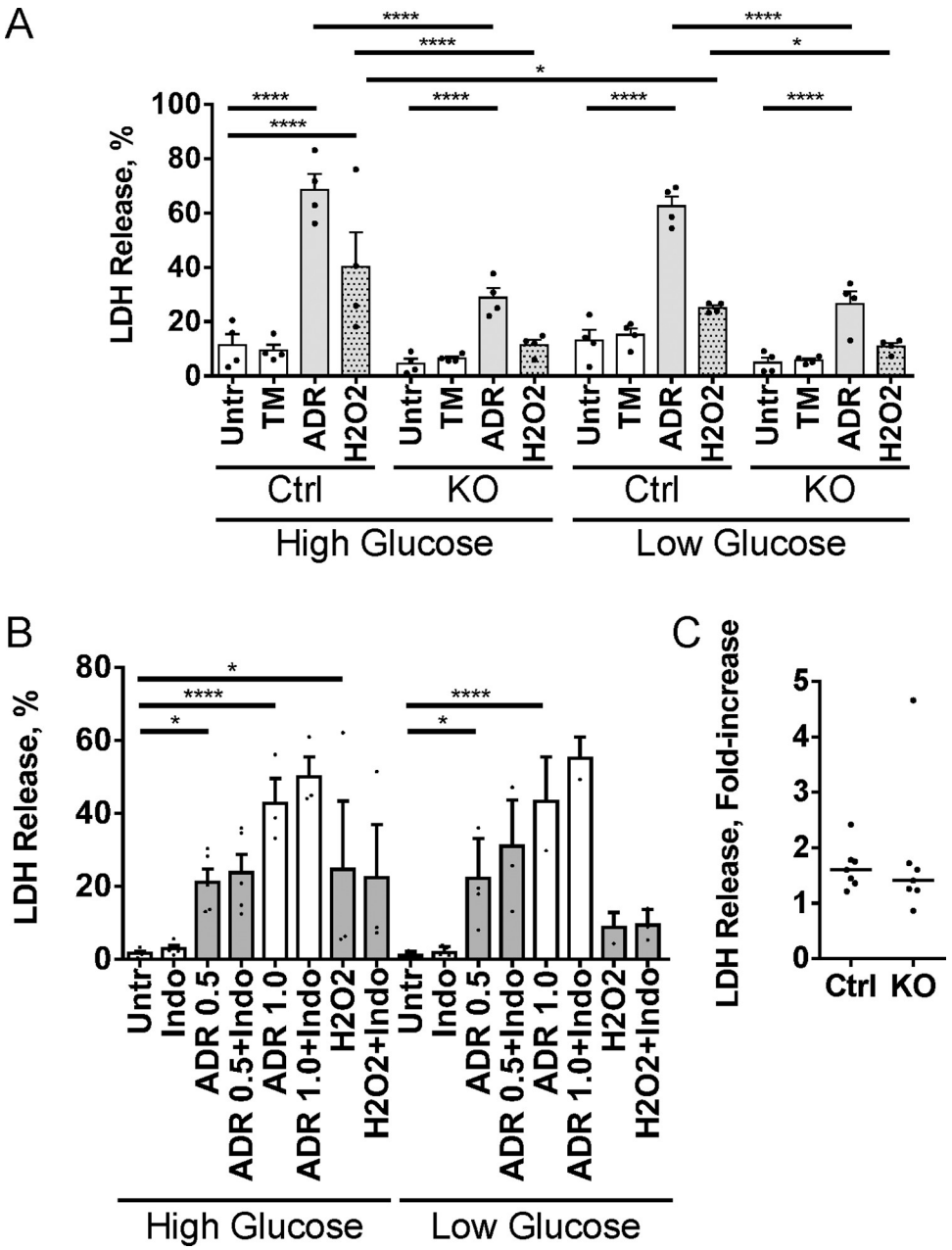

Fig 6. Control (Ctrl) GECs are more susceptible to injury compared to iPLA$_2$γ KO GECs. A) Control and iPLA$_2$γ KO GECs were untreated, or treated with tunicamycin (TM; 5 μg/ml), adriamycin (ADR; 2 μM) or H_2O_2 (1 mM) in high (36 mM) or low glucose (7.8 mM) media for 24 h. At the end of incubations, LDH was measured in cell supernatants and lysates, and percent LDH release was calculated. Control GECs are more susceptible to adriamycin- or H_2O_2-induced cytolysis compared to iPLA$_2$γ KO GECs. In control GECs, H_2O_2-induced cytolysis is greater in high glucose. 5 experiments performed in duplicate. *P<0.05, ****P<0.0001 (ANOVA). B) Control GECs (high glucose) were untreated or treated with indomethacin (Indo; 10 μM), ADR (0.5 and 1.0 μM), H_2O_2 (1 mM), ADR + Indo or H_2O_2 + Indo for 24 h. No significant effects of Indo on LDH release are observed. 3–5 experiments performed in duplicate. *P<0.05, ****P<0.0001 (ANOVA). C) Effect of autophagy inhibition on LDH release. Control and iPLA$_2$γ KO GECs were incubated with H_2O_2 (1 mM) in the presence or absence of 2.5 μM SBI0206965 for 24 h. (SBI0206965 did independently induce LDH release.) SBI0206965 augments H_2O_2-induced LDH release to a similar extent in control and iPLA$_2$γ KO GECs. Values are fold-increase in LDH release in the presence of SBI0206965 compared to its absence (bars indicate median values, P = not significant, Mann Whitney U test). LDH release after H_2O_2 treatment in the absence of SBI020696 was 9.9±2.2% in control GECs and 4.3±0.08% in iPLA$_2$γ KO GECs. 4 experiments performed in duplicate.

https://doi.org/10.1371/journal.pone.0311404.g006

into serum after a glucose challenge compared to iPLA$_2$γ global KO mice (on a standard or high fat diet). Despite these differences in serum insulin, blood glucose levels were comparable [18]. Administration of exogenous insulin lowered blood glucose to a greater extent in iPLA$_2$γ KO mice [18]. In mice with skeletal muscle deletion of iPLA$_2$, despite their resistance to developing hyperglycemia, high fat feeding did not result in significant differences in insulin levels or insulin signaling compared to control mice [19]. These results are in keeping with enhanced insulin sensitivity in iPLA$_2$ KO mice.

In the present study, morphologic changes in diabetic nephropathy were relatively mild. Both diabetic control and iPLA$_2$γ KO mice showed increases in glomerular matrix, compared to the respective untreated groups, and the increase was greater in control mice. Diabetic control mice also showed sclerotic glomeruli and glomeruli with dilated capillary loops, in keeping with glomerular hypertension. There were, however, no significant changes in podocyte number, expression of synaptopodin, nephrin and podocalyxin, or glomerular F-actin. Decreases in synaptopodin, nephrin and glomerular F-actin have been noted previously in more robust glomerular injury models [8, 32, 34]. Diabetic nephropathy may be associated with inflammatory cell infiltration of the glomeruli and interstitium [25]. Interactions between resident renal cells and macrophages change the microenvironment to a proinflammatory state, contributing to tissue damage and scarring [25, 35]. In our study, we did not observe significant infiltration of macrophages or neutrophils, suggesting that inflammation and inflammatory cytokines may have played only a minor role in glomerular injury.

The result that deletion of iPLA$_2$γ is protective in diabetic nephropathy was not anticipated, since previously, we showed that in anti-GBM nephritis and adriamycin nephrosis, glomerular injury was actually exacerbated in iPLA$_2$γ KO mice [5, 8]. To examine potential mechanisms for the reduced glomerular injury in diabetic iPLA$_2$γ KO mice, we studied pathways of protein degradation. In glomerulopathies, misfolded proteins may accumulate intracellularly under conditions of cellular stress. Both the ubiquitin-proteasome system and autophagy may be activated to degrade/clear these proteins [36]. There were no significant differences in protein ubiquitination among experimental groups, implying that ubiquitin-proteasome function was most likely unchanged. In contrast, autophagy (monitored by LC3-II and p62), was increased significantly in diabetic iPLA$_2$γ KO mice compared to untreated and diabetic controls. Increased LC3-II in untreated iPLA$_2$γ KO mice suggests that basal autophagy was enhanced in these mice. This in vivo result was recapitulated in cultured GECs, i.e. cultured iPLA$_2$γ KO cells show higher LC3-II compared to control. The findings are in keeping with our earlier studies, which showed increased autophagy in glomeruli of iPLA$_2$γ KO mice (both untreated and treated with adriamycin), and in resting iPLA$_2$γ KO GECs in culture [5, 8]. We had also shown that mitophagy is enhanced in iPLA$_2$γ KO GECs [5], which may facilitate removal of the damaged mitochondria observed in these cells. Whether endoplasmic reticulum stress is linked with enhanced autophagy in the iPLA$_2$γ KO mice will require further study.

Higher autophagy in iPLA$_2$γ KO mice may confer cytoprotection. This view is supported by studies in cultured GECs, where autophagy was cytoprotective. Indeed, autophagy is believed to be a major protective mechanism to clear misfolded proteins in podocytes [30, 36, 40]. The reason why autophagy was associated with protection from diabetic glomerular injury in iPLA$_2$γ KO mice, but was insufficient to be protective in earlier studies of iPLA$_2$γ in experimental glomerulonephritis may be related to the acuity of the injury. In anti-GBM nephritis and adriamycin nephrosis, glomerular injury occurred over the span of a few days to 4 weeks [5, 8], while in the present study, diabetic nephropathy was a chronic lesion, developing over 5–6 months. Such distinct effects of iPLA$_2$γ are perhaps not entirely surprising, since as discussed above, iPLA$_2$γ activation was shown to be both protective or deleterious depending on the pathophysiological context [8, 14–16, 21].

There has been substantial interest in the role of autophagy in the pathogenesis of experimental diabetic nephropathy; however, conflicting results have been reported, and the role of autophagy remains to be defined precisely [29, 30]. For example, in one study, the basal level of autophagy in podocytes was reduced in mice with STZ-induced diabetes [41]. In contrast, deletion of the Atg5 autophagy component in podocytes resulted in accelerated podocyte injury and albuminuria in STZ diabetic nephropathy [42]. A similar phenotype developed after deletion of Atg5 in glomerular endothelial cells. Thus, autophagy may be an important protective mechanism in both cell types of the glomerular capillary wall.

To further explore how deletion of iPLA$_2$γ may have decreased albuminuria in diabetes, additional studies were conducted in cultured GECs. To recapitulate the diabetic environment, GECs from control and iPLA$_2$γ KO mice were exposed to media with high glucose concentration. Control GECs were more susceptible to adriamycin- or H_2O_2-induced cytolysis compared to iPLA$_2$γ KO GECs, and in control GECs, H_2O_2-induced cytolysis was greater in high glucose medium. Thus, greater cytolysis in control GECs recapitulates albuminuria and podocyte injury in vivo.

Previous studies have shown that glomerular cells contain cyclooxygenase and 12/15-lipoxygenase activities [37, 38, 43], and inhibition of cyclooxygenase-2 or 12/15-lipoxygenase reduced glomerular injury in diabetic models [37, 38, 44]. Furthermore, activation of iPLA$_2$γ can lead to release of arachidonic acid and production of prostanoids in GECs [10]. Together, these results suggested that activation of iPLA$_2$γ could potentially result in the generation of cytotoxic prostanoid, lipoxygenase or HETE product(s) that could injure glomerular cells. We observed that the cyclooxygenase inhibitor indomethacin did not, however, reduce cytotoxicity in control GECs. The 12/15-lipoxygenase inhibitor baicalein reversed H_2O_2-induced cytotoxicity, but the effect of baicalein was similar in both control and iPLA$_2$γ KO GECs. Therefore, it cannot be concluded that the cytoprotective effect of baicalein was associated with iPLA$_2$γ-dependent arachidonic acid release. Our results are similar to those in a recent study, which showed that hepatocytes from control mice were more susceptible to cytolytic injury compared to iPLA$_2$γ KO hepatocytes. However, unlike our results, cytolysis in control hepatocytes was reduced with a lipoxygenase inhibitor, most likely due to inhibition of 12-HETE production [22]. In the future, it will be necessary to identify other factors that may be differentially regulated by iPLA$_2$γ and hyperglycemia in glomeruli. For example, in mitochondria under stress, cytochrome c may oxidize polyunsaturated fatty acyl chains in cardiolipin. Then, iPLA$_2$γ can hydrolyze these oxidized fatty acids. This may lead to the production of a variety of lipid-derived signaling molecules that have not been fully characterized so far [45].

There are some limitations to the present study. Deletion of iPLA$_2$γ in our mice was global and not restricted to podocytes or other glomerular cells. Thus, we cannot exclude that the primary action of iPLA$_2$γ in diabetic nephropathy occurred outside of the kidney. Nevertheless, development of albuminuria is typically associated with podocyte injury [3, 4], and mitochondrial ultrastructural damage and autophagy in iPLA$_2$γ KO mice were present only in podocytes, and no other glomerular cells or proximal tubular cells [8]. Results of studies of diabetes in cultured GECs have not been consistent. In one study, high glucose concentrations promoted autophagy [42], but in another, high glucose reduced the levels of autophagy markers [41]. Studies in cultured GECs may not accurately reflect the diabetic environment in vivo, and more complex cell culture models, e.g. co-culture of cell lines, may be required to address mechanistic questions [46]. Evaluation of iPLA$_2$γ metabolic effects and autophagy in human diabetic kidneys is difficult, although autophagy genes and gene ontology pathways are upregulated in glomeruli in human diabetic nephropathy [47].

In conclusion, this and other studies support a protective role for autophagy in diabetic nephropathy, and suggest that autophagy could be an attractive therapeutic target in human

disease. The precise molecular pathway(s) of iPLA$_2$γ that mediate glomerular damage require further identification in future studies.

Supporting information

S1 Fig. Blood glucose and body weights of mice. A) STZ induces significant increases in blood glucose in both control and iPLA$_2$γ KO mice; glucose levels are higher in control mice. N = 9 mice in control (Ctrl) untreated (Untr), 10 in KO Untr, 10 in Ctrl STZ and 15 in KO STZ groups. B) Blood glucose levels after removal of the 7 STZ-treated KO mice with smaller increases in blood glucose levels (N = 8). C) Untreated and STZ-treated KO mice show lower body weights compared to untreated and STZ-treated controls. STZ-treated control mice show lower body weight compared to untreated control. D) Body weights after removal of the 7 STZ-treated mice with smaller increases in blood glucose. The glucose and body weights of each mouse represent mean values over the study period. *P<0.05, ***P<0.001, ****P<0.0001 (ANOVA). Since the blood glucose data in the Ctrl STZ and Ctrl groups was not normally distributed (panels A and B), we also used the Kruskal-Wallis test to confirm significant differences among groups (p<0.0001).
(PDF)

S2 Fig. KO of iPLA$_2$γ attenuates development of albuminuria in STZ-induced diabetic nephropathy. See legend to Fig 1. Results are presented after removal of 7 STZ-treated KO mice with smaller increases in blood glucose (N = 8 in KO STZ). The statistical significance of the changes remains the same as in Fig 1.
(PDF)

S3 Fig. Expression of glomerular structural proteins in diabetic nephropathy. Glomerular lysates were immunoblotted with antibodies as indicated. Signals were quantified by densitometry. Bars indicate median values. There are no significant differences in nephrin and podocalyxin (Podocal) expression among groups (Kruskal-Wallis). There are 6–8 mice per group.
(PDF)

S4 Fig. Glomerular F-actin content. Kidney sections were stained with FITC-phalloidin, which reflects F-actin, and antibody to synaptopodin. A and B) Representative fluorescence micrographs and quantification of FITC-phalloidin fluorescence intensity are shown. Quantification of synaptopodin immunofluorescence intensity is similar to Fig 4. There are no significant differences in fluorescence intensity among groups. Pearson correlation coefficient for phalloidin and synaptopodin. There are no significant differences among groups (ANOVA or Kruskal-Wallis). 2–8 glomeruli/mouse in 4 mice per group were analyzed. Bar = 25 μm.
(PDF)

S5 Fig. Renal macrophage infiltration. Kidney sections were stained with F4/80 antibody, which identifies macrophages. Representative micrographs are presented. There is only minimal F4/80 staining in the kidneys in the four groups of mice. Spleen is presented as positive control. Kidneys of 4–6 mice per group were examined. Bars = 80 μm.
(PDF)

S6 Fig. Glomerular neutrophil infiltration. Kidney sections were stained with periodic acid-Schiff. Photomicrographs of diabetic control and KO mice showing neutrophils are presented. The neutrophils are labelled with arrows. Kidneys of 5–6 mice per group were examined. Bar = 30 μm.
(PDF)

S7 Fig. Production of reactive oxygen species in GECs. Total reactive oxygen species in control and iPLA$_2$γ KO GECs were monitored by 2',7'-dichlorodihydrofluorescein diacetate (DCF) staining. GECs were cultured in media containing high (36 mM) or low glucose (7.8 mM) plus mannitol for 24 h. DCF was added and fluorescence was measured after 15 min. There are no significant differences in DCF fluorescence between high and low glucose groups, nor between control and iPLA$_2$γ KO GECs (ANOVA). 6 experiments.
(PDF)

S8 Fig. Autophagy in GECs. A and B) Control and iPLA$_2$γ KO GECs were cultured in medium containing 7.8 mM glucose (Glu). Then, medium was switched to 7.8 mM glucose + 28 mM mannitol (Man) or high glucose (36 mM), and cells were treated with or without chloroquine (CQ; 25 μM) for 24 h. Cell lysates were immunoblotted with anti-LC3 antibody and signals were quantified by densitometry. LC3-II increases significantly after addition of CQ in control and iPLA$_2$γ KO cells exposed to mannitol or high glucose; however, there are no significant differences among the 4 CQ-treated groups. *P<0.05, **P<0.01, ***P<0.001 (ANOVA). 4 experiments performed in duplicate (ANOVA). C and D) Control GECs were untreated (U) or were incubated with CQ (25 μM), tunicamycin (Tun, 1 μg/ml), Tun + SAR405 (SAR, 5 or 10 μM), or Tun + SBI0206965 (SBI, 5 or 10 μM) for 24 h. Cell lysates were immunoblotted as above. Tun increases LC3-II and the increase is blocked by SBI0206965, but not SAR405. **P<0.01 (ANOVA). 4 experiments performed in duplicate.
(PDF)

S1 Raw images. Uncropped immunoblots.
(PDF)

S1 Data. Primary data.
(XLSX)

Author Contributions

Conceptualization: Andrey V. Cybulsky, I. George Fantus.

Data curation: Andrey V. Cybulsky.

Formal analysis: Andrey V. Cybulsky, I. George Fantus.

Funding acquisition: Andrey V. Cybulsky.

Investigation: Andrey V. Cybulsky, Joan Papillon, Julie Guillemette, José R. Navarro-Betancourt, Hanan Elimam.

Methodology: Andrey V. Cybulsky, Joan Papillon, Julie Guillemette, José R. Navarro-Betancourt, Hanan Elimam.

Project administration: Andrey V. Cybulsky.

Resources: Andrey V. Cybulsky.

Supervision: Andrey V. Cybulsky.

Validation: Andrey V. Cybulsky.

Writing – original draft: Andrey V. Cybulsky.

Writing – review & editing: Andrey V. Cybulsky, Joan Papillon, Julie Guillemette, José R. Navarro-Betancourt, Hanan Elimam, I. George Fantus.

References

1. KDIGO. Kidney Disease: Improving Global Outcomes (KDIGO) Glomerulonephritis Work Group. KDIGO clinical practice guideline for glomerulonephritis. Kidney Int Suppl. 2012; 2: 139–274.
2. Rossing P, Caramori ML, Chan JCN, Heerspink HJL, Hurst C, Khunti K, et al. Executive summary of the KDIGO 2022 clinical practice guideline for diabetes management in chronic kidney disease: an update based on rapidly emerging new evidence. Kidney Int. 2022; 102: 990–999. https://doi.org/10.1016/j.kint.2022.06.013 PMID: 36272755
3. Pavenstadt H, Kriz W, Kretzler M. Cell biology of the glomerular podocyte. Physiol Rev. 2003; 83: 253–307. https://doi.org/10.1152/physrev.00020.2002 PMID: 12506131
4. Greka A, Mundel P. Cell biology and pathology of podocytes. Annu Rev Physiol. 2012; 74: 299–323. https://doi.org/10.1146/annurev-physiol-020911-153238 PMID: 22054238
5. Elimam H, Papillon J, Guillemette J, Navarro-Betancourt JR, Cybulsky AV. Genetic ablation of calcium-independent phospholipase A2gamma exacerbates glomerular injury in adriamycin nephrosis in mice. Sci Rep. 2019; 9: 16229.
6. Hara S, Yoda E, Sasaki Y, Nakatani Y, Kuwata H. Calcium-independent phospholipase A(2)gamma (iPLA(2)gamma) and its roles in cellular functions and diseases. Biochim Biophys Acta Mol Cell Biol Lipids. 2019; 1864: 861–868.
7. Cohen D, Papillon J, Aoudjit L, Li H, Cybulsky AV, Takano T. Role of calcium-independent phospholipase A2 in complement-mediated glomerular epithelial cell injury. Am J Physiol Renal Physiol. 2008; 294: F469–479. https://doi.org/10.1152/ajprenal.00372.2007 PMID: 18171998
8. Elimam H, Papillon J, Kaufman DR, Guillemette J, Aoudjit L, Gross RW, et al. Genetic ablation of calcium-independent phospholipase A2gamma induces glomerular injury in mice. J Biol Chem. 2016; 291: 14468–14482.
9. Cummings BS, McHowat J, Schnellmann RG. Role of an endoplasmic reticulum Ca(2+)-independent phospholipase A(2) in oxidant-induced renal cell death. Am J Physiol Renal Physiol. 2002; 283: F492–498. https://doi.org/10.1152/ajprenal.00022.2002 PMID: 12167600
10. Elimam H, Papillon J, Takano T, Cybulsky AV. Complement-mediated activation of calcium-independent phospholipase A2gamma: role of protein kinases and phosphorylation. J Biol Chem. 2013; 288: 3871–3885.
11. Kinsey GR, McHowat J, Beckett CS, Schnellmann RG. Identification of calcium-independent phospholipase A2gamma in mitochondria and its role in mitochondrial oxidative stress. Am J Physiol Renal Physiol. 2007; 292: F853–860. https://doi.org/10.1152/ajprenal.00318.2006 PMID: 17047165
12. Jezek J, Jaburek M, Zelenka J, Jezek P. Mitochondrial phospholipase A2 activated by reactive oxygen species in heart mitochondria induces mild uncoupling. Physiol Res. 2010; 59: 737–747. https://doi.org/10.33549/physiolres.931905 PMID: 20406040
13. Elimam H, Papillon J, Takano T, Cybulsky AV. Calcium-independent phospholipase A2gamma enhances activation of the ATF6 transcription factor during endoplasmic reticulum stress. J Biol Chem. 2015; 290: 3009–3020.
14. Moon SH, Jenkins CM, Kiebish MA, Sims HF, Mancuso DJ, Gross RW. Genetic ablation of calcium-independent phospholipase A(2)gamma (iPLA(2)gamma) attenuates calcium-induced opening of the mitochondrial permeability transition pore and resultant cytochrome c release. J Biol Chem. 2012; 287: 29837–29850.
15. Mancuso DJ, Sims HF, Han X, Jenkins CM, Guan SP, Yang K, et al. Genetic ablation of calcium-independent phospholipase A2gamma leads to alterations in mitochondrial lipid metabolism and function resulting in a deficient mitochondrial bioenergetic phenotype. J Biol Chem. 2007; 282: 34611–34622. https://doi.org/10.1074/jbc.M707795200 PMID: 17923475
16. Mancuso DJ, Kotzbauer P, Wozniak DF, Sims HF, Jenkins CM, Guan S, et al. Genetic ablation of calcium-independent phospholipase A2{gamma} leads to alterations in hippocampal cardiolipin content and molecular species distribution, mitochondrial degeneration, autophagy, and cognitive dysfunction. J Biol Chem. 2009; 284: 35632–35644. https://doi.org/10.1074/jbc.M109.055194 PMID: 19840936
17. Yoda E, Hachisu K, Taketomi Y, Yoshida K, Nakamura M, Ikeda K, et al. Mitochondrial dysfunction and reduced prostaglandin synthesis in skeletal muscle of Group VIB Ca2+-independent phospholipase A2gamma-deficient mice. J Lipid Res. 2010; 51: 3003–3015. https://doi.org/10.1194/jlr.M008060 PMID: 20625036
18. Mancuso DJ, Sims HF, Yang K, Kiebish MA, Su X, Jenkins CM, et al. Genetic ablation of calcium-independent phospholipase A2gamma prevents obesity and insulin resistance during high fat feeding by mitochondrial uncoupling and increased adipocyte fatty acid oxidation. J Biol Chem. 2010; 285: 36495–36510. https://doi.org/10.1074/jbc.M110.115766 PMID: 20817734

19. Moon SH, Dilthey BG, Guan S, Sims HF, Pittman SK, Keith AL, et al. Genetic deletion of skeletal muscle iPLA(2)gamma results in mitochondrial dysfunction, muscle atrophy and alterations in whole-body energy metabolism. iScience. 2023; 26: 106895.

20. Moon SH, Mancuso DJ, Sims HF, Liu X, Nguyen AL, Yang K, et al. Cardiac myocyte-specific knock-out of calcium-independent phospholipase A2gamma (iPLA2gamma) decreases oxidized fatty acids during ischemia/reperfusion and reduces infarct size. J Biol Chem. 2016; 291: 19687–19700.

21. Moon SH, Liu X, Cedars AM, Yang K, Kiebish MA, Joseph SM, et al. Heart failure-induced activation of phospholipase iPLA(2)gamma generates hydroxyeicosatetraenoic acids opening the mitochondrial permeability transition pore. J Biol Chem. 2018; 293: 115–129.

22. Moon SH, Dilthey BG, Liu X, Guan S, Sims HF, Gross RW. High-fat diet activates liver iPLA(2)gamma generating eicosanoids that mediate metabolic stress. J Lipid Res. 2021; 62: 100052.

23. Burnyte B, Vilimiene R, Grigalioniene K, Adomaitiene I, Utkus A. Cerebellar ataxia and peripheral neuropathy in a family with pnpla8-associated disease. Neurol Genet. 2023; 9: e200068. https://doi.org/10.1212/NXG.0000000000200068 PMID: 37057294

24. Abdel-Hamid MS, Abdel-Salam GMH, Abdel-Ghafar SF, Zaki MS. Delineating the phenotype of PNPLA8-related mitochondriopathies. Clin Genet. 2024; 105: 92–98. https://doi.org/10.1111/cge.14421 PMID: 37671596

25. Thomas MC, Brownlee M, Susztak K, Sharma K, Jandeleit-Dahm KA, Zoungas S, et al. Diabetic kidney disease. Nat Rev Dis Primers. 2015; 1: 15018. https://doi.org/10.1038/nrdp.2015.18 PMID: 27188921

26. Alicic RZ, Rooney MT, Tuttle KR. Diabetic kidney disease: challenges, progress, and possibilities. Clin J Am Soc Nephrol. 2017; 12: 2032–2045. https://doi.org/10.2215/CJN.11491116 PMID: 28522654

27. Azushima K, Gurley SB, Coffman TM. Modelling diabetic nephropathy in mice. Nat Rev Nephrol. 2018; 14: 48–56. https://doi.org/10.1038/nrneph.2017.142 PMID: 29062142

28. Alpers CE, Hudkins KL. Mouse models of diabetic nephropathy. Curr Opin Nephrol Hypertens. 2011; 20: 278–284. https://doi.org/10.1097/MNH.0b013e3283451901 PMID: 21422926

29. Zhuang A, Forbes JM. Stress in the kidney is the road to pERdition: is endoplasmic reticulum stress a pathogenic mediator of diabetic nephropathy? J Endocrinol. 2014; 222: R97–111. https://doi.org/10.1530/JOE-13-0517 PMID: 24982467

30. Tang C, Livingston MJ, Liu Z, Dong Z. Autophagy in kidney homeostasis and disease. Nat Rev Nephrol. 2020; 16: 489–508. https://doi.org/10.1038/s41581-020-0309-2 PMID: 32704047

31. Furman BL. Streptozotocin-induced diabetic models in mice and rats. Curr Protoc Pharmacol. 2015; 70: 5 47 41–20. https://doi.org/10.1002/0471141755.ph0547s70 PMID: 26331889

32. Navarro-Betancourt JR, Papillon J, Guillemette J, Iwawaki T, Chung CF, Cybulsky AV. Role of IRE1alpha in podocyte proteostasis and mitochondrial health. Cell Death Discov. 2020; 6: 128.

33. Navarro-Betancourt JR, Papillon J, Guillemette J, Iwawaki T, Chung CF, Cybulsky AV. The unfolded protein response transducer IRE1alpha promotes reticulophagy in podocytes Biochim Biophys Acta Mol Basis Dis. 2022; 1868: 166391.

34. Xu W, Ge Y, Liu Z, Gong R. Glycogen synthase kinase 3beta dictates podocyte motility and focal adhesion turnover by modulating paxillin activity: implications for the protective effect of low-dose lithium in podocytopathy. Am J Pathol. 2014; 184: 2742–2756.

35. Tessaro FH, Ayala TS, Martins JO. Lipid mediators are critical in resolving inflammation: a review of the emerging roles of eicosanoids in diabetes mellitus. Biomed Res Int. 2015; 2015: 568408. https://doi.org/10.1155/2015/568408 PMID: 25866794

36. Cybulsky AV. Endoplasmic reticulum stress, the unfolded protein response and autophagy in kidney diseases. Nat Rev Nephrol. 2017; 13: 681–696. https://doi.org/10.1038/nrneph.2017.129 PMID: 28970584

37. Ma J, Natarajan R, LaPage J, Lanting L, Kim N, Becerra D, et al. 12/15-lipoxygenase inhibitors in diabetic nephropathy in the rat. Prostaglandins Leukot Essent Fatty Acids. 2005; 72: 13–20. https://doi.org/10.1016/j.plefa.2004.06.004 PMID: 15589395

38. Xu HZ, Cheng YL, Wang WN, Wu H, Zhang YY, Zang CS, et al. 12-Lipoxygenase inhibition on microalbuminuria in type-1 and type-2 diabetes is associated with changes of glomerular angiotensin ii type 1 receptor related to insulin resistance. Int J Mol Sci. 2016; 17: https://doi.org/10.3390/ijms17050684 PMID: 27164093

39. Klionsky DJ, Abdel-Aziz AK, Abdelfatah S, Abdellatif M, Abdoli A, Abel S, et al. Guidelines for the use and interpretation of assays for monitoring autophagy (4th edition). Autophagy. 2021; 17: 1–382.

40. Huber TB, Edelstein CL, Hartleben B, Inoki K, Jiang M, Koya D, et al. Emerging role of autophagy in kidney function, diseases and aging. Autophagy. 2012; 8: 1009–1031. https://doi.org/10.4161/auto.19821 PMID: 22692002

41. Fang L, Zhou Y, Cao H, Wen P, Jiang L, He W, et al. Autophagy attenuates diabetic glomerular damage through protection of hyperglycemia-induced podocyte injury. PLoS One. 2013; 8: e60546. https://doi.org/10.1371/journal.pone.0060546 PMID: 23593240

42. Lenoir O, Jasiek M, Henique C, Guyonnet L, Hartleben B, Bork T, et al. Endothelial cell and podocyte autophagy synergistically protect from diabetes-induced glomerulosclerosis. Autophagy. 2015; 11: 1130–1145. https://doi.org/10.1080/15548627.2015.1049799 PMID: 26039325

43. Takano T, Cybulsky AV. Complement C5b-9-mediated arachidonic acid metabolism in glomerular epithelial cells: role of cyclooxygenase-1 and -2. Am J Pathol. 2000; 156: 2091–2101. https://doi.org/10.1016/S0002-9440(10)65080-8 PMID: 10854230

44. Cheng H, Fan X, Moeckel GW, Harris RC. Podocyte COX-2 exacerbates diabetic nephropathy by increasing podocyte (pro)renin receptor expression. J Am Soc Nephrol. 2011; 22: 1240–1251. https://doi.org/10.1681/ASN.2010111149 PMID: 21737546

45. Kagan VE, Tyurin VA, Jiang J, Tyurina YY, Ritov VB, Amoscato AA, et al. Cytochrome c acts as a cardiolipin oxygenase required for release of proapoptotic factors. Nat Chem Biol. 2005; 1: 223–232. https://doi.org/10.1038/nchembio727 PMID: 16408039

46. Albrecht M, Sticht C, Wagner T, Hettler SA, De La Torre C, Qiu J, et al. The crosstalk between glomerular endothelial cells and podocytes controls their responses to metabolic stimuli in diabetic nephropathy. Sci Rep. 2023; 13: 17985. https://doi.org/10.1038/s41598-023-45139-7 PMID: 37863933

47. Chung CF, Papillon J, Navarro-Betancourt JR, Guillemette J, Bhope A, Emad A, et al. Analysis of gene expression and use of connectivity mapping to identify drugs for treatment of human glomerulopathies. Front Med. 2023; 10: 1122328. https://doi.org/10.3389/fmed.2023.1122328 PMID: 36993805